Spatio-temporal Artifact Correction of Multi-dimensional Spectroscopic Imaging Data
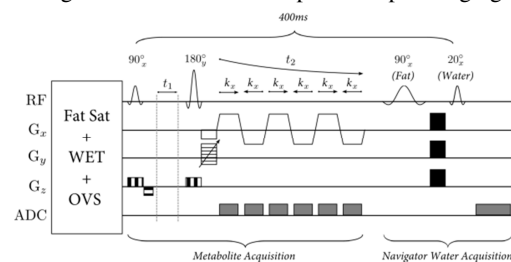
Brian Burns[1], Neil Wilson[2], and M. Albert Thomas[2,3]

[1]Department of Bioengineering, UCLA, Los Angeles, CA, United States, [2]Medical Physics, IDP, UCLA, Los Angeles, CA, United States, [3]Department of Radiology, UCLA, Los Angeles, CA, United States

Intended Audience: Researchers working in phase error correction and pulse sequence programming of multi-dimensional spectroscopic imaging.

Purpose: Numerous sources of spatial-spectral phase errors exist in multi-dimensional spectroscopic imaging (MRSI). Current phase correction techniques do not take into account the spatio-temporally coupled nature of these errors because they were designed for single voxel methods[1]. This work categorizes phase errors in 4D MRSI (2D spatial+2D spectral) as time varying, $B_0(t)$, space varying, $B_0(x,y)$, or space and time varying, $B_0(x,y,t)$, and proposes a post-processing pipeline that decouples these phase errors so they can be removed in the appropriate domain. The 4D Interleaved Navigator Scan corrected Echo Planar J-Resolved Spectroscopic Imaging (INSEP-JRESI) sequence is proposed, which incorporates an interleaved navigator scan (INS) into each TR to track $B_0(t)$ field drifts and off-resonance effects[2]. Results from gray matter phantom scans using the INSEP-JRESI sequence and new pipeline are compared to those processed by an MRSI adapted Klose's method (AKM)[1,3]. These results show the new pipeline produces metabolite peak amplitudes up to 10% higher with improved line-shapes and spatial distributions compared to AKM.
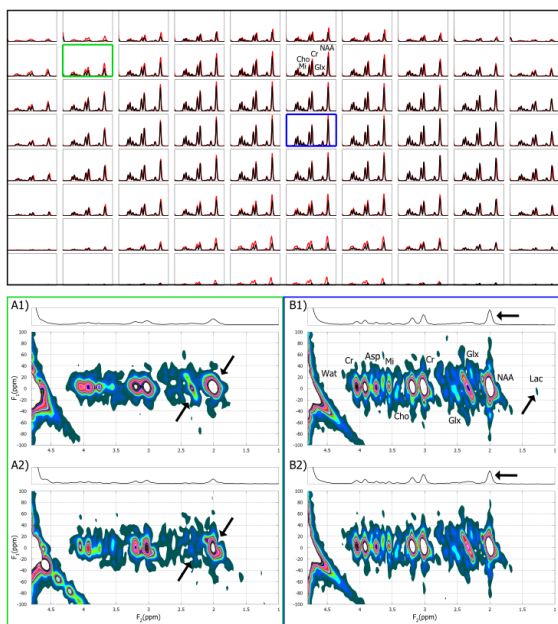

Figure 1: A single TR of the 4D INSEP-JRESI pulse sequence with interleaved navigator scan.

Table 1: Mean metabolite peak amplitudes and FWHM along F_1 and F_2 for both processing methods.

	Amplitude		F_1 FWHM		F_2 FWHM	
	mean	CV (%)	mean (Hz)	CV (%)	mean (Hz)	CV (%)
Klose's Method Post-Processing						
NAA (2.0ppm)	2.669	40.5	6.989	3.97	8.932	36.6
Glx (2.2ppm)	0.434	31.7	7.205	15.1	8.749	33.1
Cr (3.0ppm)	2.017	40.4	7.006	5.6	8.716	34.0
Cho (3.2ppm)	1.355	37.1	7.189	13.6	9.596	45.4
mI (3.5ppm)	0.547	33.2	7.238	14.9	9.778	40.7
Cr (3.9ppm)	0.978	39.5	7.172	15.3	9.695	49.2
INSEP-JRESI Post-Processing						
NAA (2.0ppm)	2.952	36.4	6.973	0.0	8.417	28.4
Glx (2.2ppm)	0.463	30.0	7.255	16.3	8.417	28.4
Cr (3.0ppm)	2.098	37.5	6.973	0.0	8.45	30.7
Cho (3.2ppm)	1.413	31.7	6.973	0.0	9.015	33.4
mI (3.5ppm)	0.561	31.3	7.006	5.6	9.712	40.5
Cr (3.9ppm)	0.989	36.8	6.989	4.0	8.948	40.4

Methods: The INSEP-JRESI pulse sequence shown in Fig. 1 is derived from 4D EP-JRESI[3]. The 20° flip angle excite-acquire INS in INSEP-JRESI occurs 400ms after the metabolite excitation to allow the water signal to regrow after WET water suppression. No spatial encoding or slice selection is used for the INS acquisition, which uses a 1 kHz spectral bandwidth (256 samples). A spectrally selective 90° pulse at 0.3ppm with a bandwidth of 2ppm followed by dephasing crushers suppresses fat prior to the INS. The new multi-step processing pipeline: **1)** estimates and remove off-resonance and $B_0(t)$ field drift at each TR using an adapted Dynamic Off-resonance in k-space (DORK) technique[4] **2)** even-odd echoes along the $\mathbf{k_x}\text{-}\mathbf{t_2}$ readout are phase aligned by applying a $\mathbf{k_x}$ dependent phase-shift along $\mathbf{F_2}$ to each even echo post flip: $\Delta\varphi_{m,n} = e^{2\pi i \cdot f_m \Delta t_n}$ where Δt_n is the delay incurred at the nth $\mathbf{k_x}$ point and m^{th} $\mathbf{F_2}$ frequency point[5] **3)** $B_0(x,y,t)$ eddy currents are removed in k-space using modified Interleaved Dual-Echo Acceleration Echo Planar Imaging (IDEA-EPI) with complex echo averaging[6] **4)** $B_0(x,y)$ 0th order phase offsets from the phased array coils are removed in the spatial domain by standard first point methods[3]. Seven INSEP-JRESI gray matter brain phantom scans were acquired for this work using a 12-channel head phased array coil with these parameters: TR/TE=1.7s/13ms, 16x16 FOV, 1x1x1.5cm³ voxels, and F_1/F_2 spectral bandwidths=1250/1190Hz (100 t_1/256 t_2 points). The total scan time was 45 minutes.

Results: Fig. 2 shows a representative gray matter phantom scan that has been processed using the new pipeline or AKM. 1D JPRESS spectra from F_1=0 in the top, show the scan processed by AKM has lower metabolite peak amplitudes with greater spatial variation. 2D JPRESS spectra in the bottom show the scan processed using the new pipeline has higher metabolite peak amplitudes, improved line-shapes, and fewer peak distortions. Table 1 shows the mean metabolite peak amplitudes and Full-Width Half-Maxima (FWHM) calculated over 40 voxels of the seven gray matter phantom scans. The largest mean peak amplitude and lowest FWHM along each spectral dimension are highlighted. All but one of the values is from the new pipeline, which is in agreement with Fig. 2.

Discussion: A new phase error correction pipeline has been developed for 4D MRSI data that decouples time, space, and spatio-temporal phase errors and corrects them in a multi-step process in the appropriate domain. Results for the new pipeline were compared against AKM in phantom, which showed the new technique resulted in higher metabolite peak amplitudes without increasing the noise floor, a more even spatial distribution of metabolite peaks, and improved line-shapes in voxels near the edges of the phantom.

Conclusion: These preliminary results show this novel post-processing method can successfully remove coupled phase errors from 4D EP-JRESI data. They show it is a viable alternative to AKM for 4D MRSI data and that it is possible to correct phase errors within the domain in which they occur. Further work is required to optimize the INSEP-JRESI navigator scan parameters and to improve the fat suppression techniques *in vivo*.

Figure 2: Gray matter phantom results from the new pipeline and AKM. (Top) Spatial distribution of 1D F_2 spectra taken from F_1=0 for new pipeline in red and AKM in black. (Bottom) JPRESS spectra from the edge and center of phantom for new pipeline (A1/B1) and AKM (A2/B2).

References: [1] U. Klose, MRM, vol. 14, 1990 [2] A. Ebel et al, MRM, vol. 53, 2005 [3] R. Nagarajan et al, 2011 ISMRM, [4] J. Pfeuffer et al, MRM, vol. 47, 2002. [5] S. Posse et al, Radiology, vol. 192, 1994. [6] B. Poser et al, MRM, vol. 69, 2013